Elucidating the catalytic effect of metal ions in montmorillonite on thermal degradation of organic modifier

Indraneel S Zope[1], Aravind Dasari[1,*], Giovanni Camino[2]

[1]School of Materials Science & Engineering (Blk N4.1), Nanyang Technological University, 50 Nanyang Avenue, Singapore 639798

[2]Dipartimento di Scienza Applicata e Tecnologia, Politecnico di Torino sede di Alessandria, INSTM research unit, Viale Teresa Michel 5, 15100 Alessandria, Italy

KEYWORDS: ignition, catalytic effect, metal-ion exchanged, montmorillonite, flame retardancy

ABSTRACT: A key parameter influencing ignition, heat of combustion and charring of polymer/clay (montmorillonite, MMT) nanocomposites during combustion is the catalytic activity of MMT. This work deals with exploring the effect of metal ions (MIs) like Mg^{2+}, Al^{3+} and Fe^{3+} that are inherent to clay in altering the kinetics of degradation of organic modifier, hexadecyltrimethylammonium bromide (HDTMA-Br). The catalytic activity was seen to be a combined effect of Brønsted and Lewis acid characters associated with the metal ions; Brønsted acidity affected the initial stages of organic modifier degradation, while Lewis acidity affected the oxidation stability of carbonaceous residue beyond dehydration temperatures. The effect varied significantly with the predominant cation in organically modified MI-clays (OMI-clays). For example, OMgMMT yielded delayed

peak degradation for $HDTMA^+$, while Fe^{3+} ions from OFeMMT significantly lowered the oxidation stability of carbonaceous content. Knowing the effect of each metal ion separately, correlation between clay structural chemistry and organic degradation onset has been established. Besides, mechanisms of degradation were provided adding fundamental knowledge to the field that will help in the design and development of polymer/clay nanocomposites with superior fire retardancy.

*Corresponding author:

E-mail: aravind@ntu.edu.sg; Fax: +65-6790 9081

HIGHLIGHTS

- Thermo-oxidative degradation of metal ion exchanged organo montmorillonite.
- Analysis of ionic character and polarizing capacity of metal ions.
- Proposed degradation mechanisms.

INTRODUCTION

Polymer/clay nanocomposites, generally exhibit lower heat release rates, but inherently lack the resistance towards quicker ignition during combustion. Many attempts were made to understand this behavior from different (and broad) perspectives including thermal stability of organic surfactants [1,2], 'barrier effect' as a result of collapse of nanoparticle structures [3,4], catalytic effect of clay on polymer matrix degradation [5-10], and heat transfer through cross-section by thermal conduction [11,12]. With many possible explanations put forth, general consensus is yet to be attained.

As well known, uniqueness of smectite clay (for example, MMT) structure comes from its negatively charged surface stabilized by relatively mobile and exchangeable cationic species like Na^{+} or Ca^{2+}. Replacing Na^{+} by higher valency metal ions like Mg^{2+}, Zn^{2+}, Cu^{2+}, Al^{3+} or Fe^{3+} will influence the relative reactivity of MMT [13]. This ability has been widely exploited for applications like catalysis [14,15]. Depending on their locations, metal ions render inherent acidic nature to MMT in the form of Brønsted acidity and Lewis acidity [13]. For polyamide 6/MMT nanocomposite system, Davis et al. argued that during processing at 300 ^{o}C, degradation of polyamide 6 possibly occurred because of peptide bond scission as a result of hydrolysis led by bound water molecules from MMT, essentially Brønsted acidolysis [6]. It was also proposed that free water by itself might not result in substantial degradation of polyamide 6 matrix, but the combination of clay and water is required for significant catalytic degradation. Lewis acidity has also been studied for its possible effect on catalytic degradation and carbonization of organic content. Dong et al. studied polystyrene/zeolite nanocomposites for which enhanced char formation was observed when zeolite with higher Lewis acidity was used in conjunction with intumescent fillers [16]. This effect was attributed to Lewis acid sites in zeolites which were argued to alter the degradation route of the matrix assisting into carbonization [16]. However, the precise role of different metal ions present in the clay structure on decomposition of organic matter is still unclear.

Further, organically modified MMT upon degradation leaves behind H^{+} at exchange position following the well accepted Hoffmann degradation mechanism. Acid activated MMT demonstrates a physical process commonly known as *autotransformation* [17].

This process can be described as migration of protons from exchange locations to replace metal ions from structural positions in tetrahedral layers. Migration of Al^{3+} in case of acid activated MMTs is well reported [18]. These "knocked-off" metal ions like Al^{3+} then assume positions at exchange sites increasing the reactivity of clay towards molten polymer matrix. Increased catalytic activities of acid treated tetra-alkyl-ammonium cation exchanged smectites have already been reported [19]. Thus, possibility of increasing concentration of metal ions like Mg^{2+}, Al^{3+} or Fe^{3+} at exchange position beyond surfactant decomposition temperature via possible autotransformation cannot be overlooked. Although control on exact kinetics of autotransformation process may not be currently feasible, knowing the effect of each metal ion on degradation kinetics of organic matter can help answer some uncertainties. Therefore, in this work, the effect of metal ions inherently present in clay on thermal degradation of organic modifier will be studied. For this, metal ion content (Mg^{2+}, Al^{3+}, Fe^{3+}) in natural sodium MMT will be amplified implementing cation exchange technique. This work forms a preliminary study of metal ion exchanged organoclays, and this knowledge subsequently will be applied towards better understanding of thermal degradation behaviors of polymer/clay nanocomposites.

Experimental Section

Materials and Synthesis Procedure

Metal ion exchanged MMT clays (MI-clays) were prepared by standard cation exchange technique. Na^+ MMT clay, commercially named *Cloisite* Na^+, was obtained

from Southern Clay Products. It has a mean formula unit of $Na_{0.65}[Al,Fe]_4Si_8O_{20}(OH)_2$ and cation exchange capacity, CEC, of 92 meq/100 g. In a typical procedure, 20 g of Na^+ MMT clay was suspended in 1 L deionized water under mechanical stirring for 24 hours. Metal salt solutions (Mg^{2+}, Al^{3+}, Fe^{3+}), 20% excess of CEC value were dissolved separately in 500 mL deionized water. MMT suspensions were heated to 80 ^oC to which metal salt solutions were added drop-wise over a period of 30 min while stirring mechanically. The suspensions were left stirring for 24 hours in order to get maximum cation exchange. Each suspension was then filtered and thoroughly washed with deionized water. Silver nitrate test for halides was conducted to confirm the thoroughness of washing. Finally, MI-clays were dried at 110 ^oC and ground into fine powder (200 mesh).

MI-clays were further modified using HDTMA-Br obtained from Sigma Aldrich. MI-clays (20 g each) were separately suspended in 1 L deionized water heated at 80 ^oC for 24 hours. Surfactant solutions were made by dissolving HDTMA-Br in 200 ml deionized water. HDTMA-Br solution was then added drop-wise to each MI-clay suspension over a period of 10 min with mechanical stirring. The suspensions were stirred for 24 hours. Each suspension was then filtered and washed thoroughly with deionized water. Silver nitrate test for bromide was also conducted to confirm the thoroughness of washing. Subsequently, these modified organo MI-clays (OMI-clays) were dried at 110 ^oC and ground to fine powder (200 mesh). Overall process is schematically represented in Figure 1.

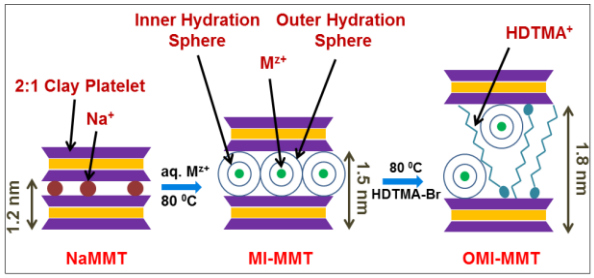

Figure 1. Schematic representation of modification of NaMMT clay to obtain MI-clays and subsequently OMI-clays, where aq. M^{z+} denotes aqueous solution of metal salts (Mg^{2+}, Al^{3+} or Fe^{3+}). Single column fitting image.

Characterization

To study the dehydration and degradation behaviors of MI- and OMI-clays, thermogravimetric (TG) analysis was carried out using TA Instruments 2950, under air and nitrogen atmospheres. All samples were dried at 110 ^{o}C for 24 hours in a convection oven before the test. Test was carried out from room temperature to 750 ^{o}C employing a heating rate of 20 ^{o}C/min. X-ray diffraction (XRD) measurements were performed on Shimadzhu XRD6000 (40kV, 30mA, Cu kα) with scan speed of 1 ^{o}/min, scan range of 3-45^{o} and step size of 0.02^{o}. Structural chemistry of clays and their residues were analyzed from respective Fourier Transform Infrared (FT-IR) spectra which were collected using Perkin Elmer SpectrumGX spectrometer and KBr disks. All spectra were acquired using 64 scans and 4 cm^{-1} resolution.

Elemental concentrations in different metal-ion exchanged clays were determined using PerkinElmer Optima2000 inductively coupled plasma optical emission

spectrometry (ICP-OES) with detectors analyzing for Na, Mg, Al and Fe. For sample preparation, accurately weighed 0.2 g of MI-clay (or OMI-clay) was dissolved in 30 mL of 1.0 M HCl for 3 hour using ultrasonic bath. The suspension was subsequently centrifuged at 6000 rpm for 5 min. Supernatant was collected into a 100 volumetric flask while settled clay was re-suspended into 30 mL of 1.0 M HCl and procedure was repeated. Upon centrifugation, the supernatant was added to earlier solution, thereafter, solution was diluted to 100 mL mark. 15 mL from this solution was used for quantifying respective ion content. Same procedure was employed to prepare test samples for all clays. PerkinElmer Series II 2400 CHNS Elementary Analyzer was used to determine carbon content in OMI-clays and their residues. All samples tested were pre-dried at 110 ^{o}C for 30 min. Carbon content values reported are averaged based on triplicate results.

RESULTS AND DISCUSSIONS

Structural aspects of MI-clays

Exchanged metal cations are known to have a profound effect on various structural aspects of MMT including changes in their basal spacing (d_{001}), interlayer water structures and their dehydration behaviors [20,21]. Their ability to form thermodynamically stable hydration complexes in presence of water has been widely reported [20]. Such hydration complexes are formed as a result of cations surrounded by coordinately bonded water molecules (schematically shown in Figure 2). They are represented as $[M^{z+}(H_2O)_6]^{z+}$ where *z* is the valency of cation *M*. Strength of these

hydration complexes is governed by the charge density of the cations present at core position (i.e., in terms of their ionic character - strength and radius, as well as polarizing power). Greater ionic character leads to stronger association, thus, requiring higher activation energy to dissociate the complex. This in turn delays their exposure to organic matter.

Apart from strength, polarizing power of cations also affects the sizes of these hydration spheres [20]. Complex shrinks in size with increase in polarizing power of cation (i.e. increasing attractive force); this is apparent from reducing distances between the metal ion and oxygen from water molecule (M-O distance) as listed in Table 1. Amongst trivalent cations, Al^{3+} and Fe^{3+} come from different rows in periodic table and inherently have different sizes, Fe > Al. This leads to variation in attractive force exerted by these trivalent cations towards oxygen resulting in slightly different M-O distance in either case. Acid dissociation values (pKa) correspond to hydrolysis reactions where proton is dissociated from metal-aqua complex. This dissociation is a complex multistage process [22, 23]. Lower pKa value for Fe^{3+} is well reported; but understanding the kinetics of dissociation reactions to completely apprehend the observations is beyond the scope of this work [22,23]. Further, instead of one hydration sphere surrounding the cation, concentric hydration spheres [24] are formed in case of polyvalent cations whose strengths are governed by their polarizing capacity. Subsequently, Na^{+} forms one hydration sphere while Mg^{2+}, Al^{3+}, and Fe^{3+} form two concentric hydration spheres, which explain observed increment in basal spacing for polyvalent MI-clays as compared to NaMMT (Table 2). XRD curves for MI-clays are provided in Supporting Information (Figure S1).

Table 1. Metal ion radius (R_i), metal ion-oxygen distance (M-O) and typical acid dissociation constants (pKa values) reported for metal ion-water complexes [23,25]. Single column fitting table.

MI-Clay	Aqua Complex	M^{z+} R_i (Å)	M-O distance (Å)	pKa
NaMMT	$[Na(H_2O)_6]^+$	1.09	2.43	13.9
MgMMT	$[Mg(H_2O)_6]^{2+}$	0.76	2.10	11.2
AlMMT	$[Al(H_2O)_6]^{3+}$	0.55	1.89	5.0
FeMMT	$[Fe(H_2O)_6]^{3+}$	0.66	2.00	2.2

However, further modification of these exchanged clays with $HDTMA^+$ resulted in similar interlayer distances in all cases irrespective of the strength and polarizing power of cations. Hence, it may be suggested that the final basal spacing is relatively independent of sizes of respective hydration spheres as a consequence of much larger size of $HDTMA^+$ compared to these hydration spheres. Basal spacings for OMI-clays are also given in Table 2 while their XRD curves are provided in Supporting Information (Figure S2). d_{001} values reported here are comparable with those reported previously [26,27].

In summary, it can be concluded that the total bound-water content for MI-clays, which in turn dictates their Brønsted acid character, is governed by polarizing capacity of each metal ion present at exchange positions.

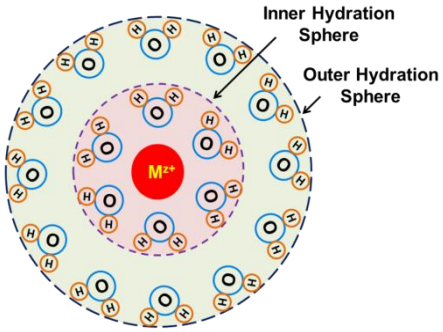

Figure 2. Schematic representation of metal-water complex [28] (M^{z+} = Na^{+}, Mg^{2+}, Al^{3+}, Fe^{3+}). Single column fitting image.

Table 2. Basal spacing for exchanged clays before and after $HDTMA^{+}$ modification. Single column fitting table.

Cation	MI-clay, in Å	OMI-clay, in Å
Na^{+}	12.1	17.5
Mg^{2+}	15.3	18.3
Al^{3+}	15.0	18.3
Fe^{3+}	15.3	17.7

Quantitative analysis of metal concentrations in MI-clays

To help correlate the magnitude of metal ions present in different exchanged clays with Brønsted and Lewis acidity and their subsequent effect on degradation of organic surfactant, ICP-OES analysis was carried out. ICP-OES results (Table 3) indicate that NaMMT inherently has varying proportions of each metal ion under consideration in this study. This suggests that any effect shown by NaMMT (or ONaMMT) can be considered as cumulative effect of all the metal ions instead of only Na^{+}. Upon exchange with

various metal ions, a clear amplification of the respective metal ion is evident. Based on the valency of metal ions exchanged, their calculated CEC values varied. Cations with higher valencies replaced those with lower valency resulting in progressively higher concentration values, which are similar to those reported previously [14,21] (Table 4). The slight variations observed in concentrations of exchanged cations can be attributed to difference in origins of sodium MMT that has been used as well as synthesis procedures implemented.

In contrast, in OMI-clays, stearic hindrance experienced by $HDTMA^+$ ions from neighboring exchange sites as a result of long organic chain can prevent complete exchange of interlayer cations by organic surfactant molecules. This results in residual irreplaceable exchangeable cations even after organic modification as seen from Table 3, which might affect degradation of surfactant or polymer matrix. Organic modification of polyvalent MI-clays using mono-valent ammonium ion can be explained further based on clay-cation preferences. As compared to larger ammonium ion in HDTMA-Br, metal ions are much smaller and possess higher aqueous-phase preference. Thermodynamically, it was also demonstrated that clay has a stronger preference to larger head-group cation, as in the case of $HDTMA^+$, which has lower aqueous-phase affinity as compared to metal ions [29]. Increasing hydrophobicity of clay surfaces results in strong repulsive forces between hydrophobic $HDTMA^+$ and water from hydration sphere surrounding the cation core. As a result, metal ions that do not have ionic bonding with clay surfaces are expelled, thus, lowering the metal ion concentrations in OMI-clays.

As mentioned before, other factors that affect the final concentration of metal ions in OMI-clays are ionic radii (R_i) and distances between metal ion and oxygen atom (M-O) from hydration sphere (see Table 1 and associated discussion). In particular, the differences between trivalent Al and Fe modifications could be explained based on their M-O distances. Smaller Al^{3+} aqua complexes readily exit the interlayer space as a result of repulsive force exerted by incoming organic cation. This is not the case with bigger Fe^{3+} aqua complexes. In fact, it was reported that they tend to precipitate in insoluble hydrous form on hydrophobic clay surfaces, in turn causing only marginal drop in final concentrations [27]. Accordingly, it was suggested that in the case of OFeMMT, precipitated hydrous Fe^{3+} repel incoming $HDTMA^+$ molecules, lowering their concentration and/or affecting their orientation at interlayer gallery. As a result of this, they displayed lower d_{001} spacing, as listed in Table 2. Concentration exceeding CEC values were also previously reported in some cases of Cu^{2+} and Fe^{3+}, but were argued to be a result of multi-nuclei complexes or colloidal particle formation[30].

Table 3. ICP-OES results showing the concentration of selected metal (ions) in NaMMT, MI clays and OMI clays (values in meq/100 g). Single column fitting table.

	Na	Mg	Al	Fe	Total CEC
NaMMT	83.0	11.3	31.9	9.4	135
ONaMMT	10.6	8.7	27.8	7.1	54

MgMMT	12.6	85.7	34.7	10.3	143
OMgMMT	9.1	15.2	28.9	7.0	60
AlMMT	12.6	6.8	131.7	9.0	160
OAlMMT	9.0	3.7	46.0	4.6	63
FeMMT	15.9	7.6	54.3	265.4	343
OFeMMT	8.9	3.5	22.1	185.0	219

Table 4. Reported metal ion concentrations (in CEC, meq/100 g) upon for cation exchanges. Single column fitting table.

Metal-ion exchanged	Obtained Results	Reported Results
Pristine clay	92	80 [14], 121 [21]
Na^{+}	83	73 [21]
Mg^{2+}	85	166 [21]
Al^{3+}	131	74 [14]
Fe^{3+}	265	198 [14]

Thermal degradation of MI clays

Brønsted Acidity in MI clays: Depending on ionic strength of cations, dehydration temperatures of different MI-clays varied as seen from Figure 3. The stronger the ion-dipole interactions, the higher are the dehydration temperatures as a consequence of higher energy required to break free the bound water. All MI-clays show intense derivative weight loss peak below 150 ^{o}C associated with free surface water evolution [21]. Beyond this temperature, MI-clays show prominent dehydration peaks up to temperatures as high as 350 ^{o}C. For example, MgMMT shows a strong shoulder between 170-210 ^{o}C; while the trivalent cation exchanged clay, FeMMT, shows much higher dehydration peak in between 180-260 ^{o}C. In case of concentric hydration spheres for polyvalent metal hydration complexes, inner hydration sphere is formed of water molecules, which are coordinately bonded with compensating cation through cation-dipole interaction. The outer hydration sphere consists of water molecules that are not directly bound to cation but have hydrogen-bonding with the inner sphere. Binding energies for inner and outer hydration spheres are reported as 19 kcal/mole and 10 kcal/mole, respectively [31,32]. Therefore, it can be argued that the dehydration of outer hydration shell starts at a lower temperature in comparison with inner shell, resulting in the observed broadening of dehydration peaks in polyvalent cations. It should be noted that as water molecules in the hydration shell experience weakening of O-H bond, this generally results in higher Brønsted acid characteristics for complexes. This Brønsted acidity, however, is a function of interlayer water and it drops sharply beyond clay dehydration temperatures. However, NaMMT does not show prominent mass loss as other MI-clays until 400 ^{o}C. It only displays minor mass loss around 265-

360 ^{o}C. But the nature of water that is responsible for this is not clear and requires more work.

Apart from dehydration temperature, cations also affect the quantity of bound water, which can be as high as 5.48 wt% [21]. In case of MI-clays, bound water content is calculated based on their respective dehydration mass loss peaks. They are found to be 1.13 wt%, 1.54 wt% and 1.25 wt% for MgMMT, AlMMT and FeMMT, respectively. In combination with high bound water content, the Brønsted acidity can play a significant role in the degradation of organic matter. The strength of Brønsted acidity as a function of polarizing power of exchangeable cations vary in the order of H^{+} > Al^{3+}, Fe^{3+} > Mg^{2+} > Na^{+}. This is further supported by the reported acid dissociation constants (Table 1). Lower value signifies easier dissociation i.e. higher acid strength. In fact, the values of Fe^{3+} and Al^{3+} water complexes are comparable to that of weak acids like acetic acid (pKa 4.76).

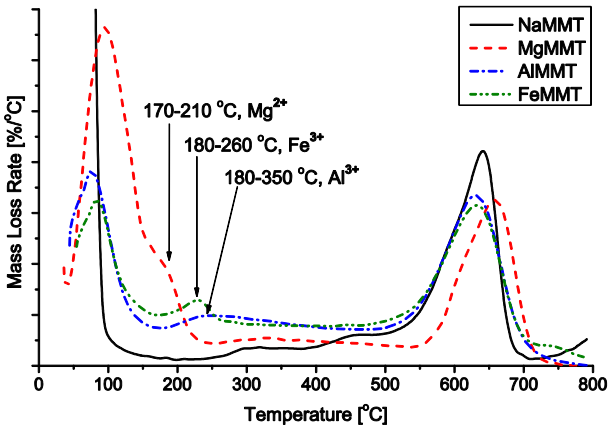

Figure 3. Mass loss rate curve for MI-clays: presence of water coordinately bonded with interlayer cations. Single column fitting image.

Lewis Acidity in MI clays: Beyond complete dehydration, exchange cations regain ionic state while at exchange positions, which otherwise were stabilized by hydration water below 300-350 ^{o}C. These exposed reactive metal ions generate Lewis sites [17,33] that can be related to Lewis acid character of clays. Here, the acidity is derived from partially bound high valence cations located at crystal edges or at defect sites. Hence, depending on inherent reactivity of exchange cations, their presence in ionic state can significantly increase overall Lewis acidity of MI-clay. Thus, such enhancements in Lewis acidity in MI-clays may help uncover effect of respective metal ions on thermo-catalytic degradation of polymer matrix or their possible effect on oxidation stability of carbonaceous char residue.

Thermal degradation analysis for OMI clays

Effect of Brønsted Acidity: To further corroborate and extend the above results, decomposition of organic modifier, HDTMA-Br, was studied under oxidative and inert conditions (Figure 4). As expected, HDTMA-Br showed comparatively quicker degradation under oxidative conditions. Onset temperature (where the mass loss reached 5 %), $T_{5\%}$, was lowered from 275 ^{o}C (in N_2 atmosphere) to 230 ^{o}C; while peak degradation temperature, T_p, reduced from 298 ^{o}C to 242 ^{o}C. Other than temperature shifts, decomposition mechanism also varied with test atmospheres. As compared to one-step decomposition at 300 ^{o}C under inert conditions, a two-step decomposition pattern was observed for oxidative conditions. The first mass loss was observed at 250 ^{o}C yielding 10 wt% residue as a result of oxidative attack on aliphatic chain in $HDTMA^{+}$

followed by complete mass loss through oxidation at 550 ^{o}C. Interestingly, these temperature regimes corresponding to onset of mass loss for organo-modifier overlap with MI-clay dehydration temperatures (Figure 3). This further increases the importance of Brønsted acid character of MI-clays towards organo-modifier decomposition.

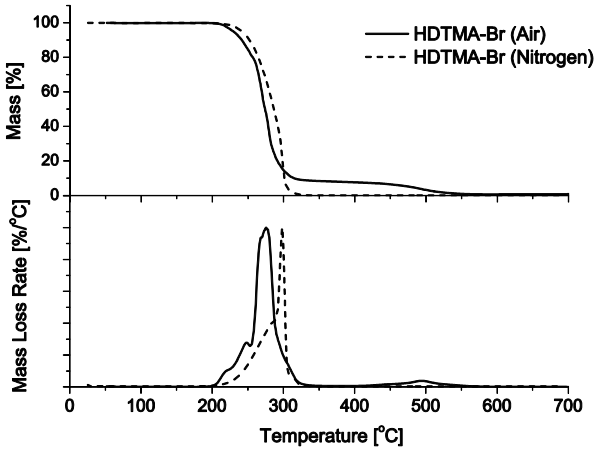

Figure 4. TG thermogram for HDTMA-Br in air and nitrogen atmosphere. Single column fitting image.

TG curves of OMI-clays under oxidative and inert atmospheres are shown in Figure 5. It is known that thermal degradation of $HDTMA^{+}$ modified clays experience two-stage decomposition process under inert conditions. Stage one typically occurs around decomposition temperature of neat surfactant (250-290 ^{o}C) and is associated with loss of surface adsorbed surfactant molecules. Second stage mass loss is observed at temperatures (~450 ^{o}C) much higher than actual decomposition temperature of surfactant. This loss is attributed to decomposition of surfactant molecules, which are

intercalated between the clay layers and can be used to quantify intercalated surfactant. Higher ionic bond strength between intercalated surfactant and clay is considered to be a prime reason for this increase in thermal stability [34]. However, a different pattern is observed when sample is tested under oxidative conditions. Although organoclays show similar mass loss trend below 300 ^{o}C, no prominent mass loss was observed between 300 ^{o}C and clay dehydroxylation temperature of 550 ^{o}C. It is argued that intercalated surfactant under oxidative conditions forms carbonaceous residue, analogous to pristine HDTMA-Br, which completely oxidizes at temperatures similar to clay dehydroxylation temperatures.

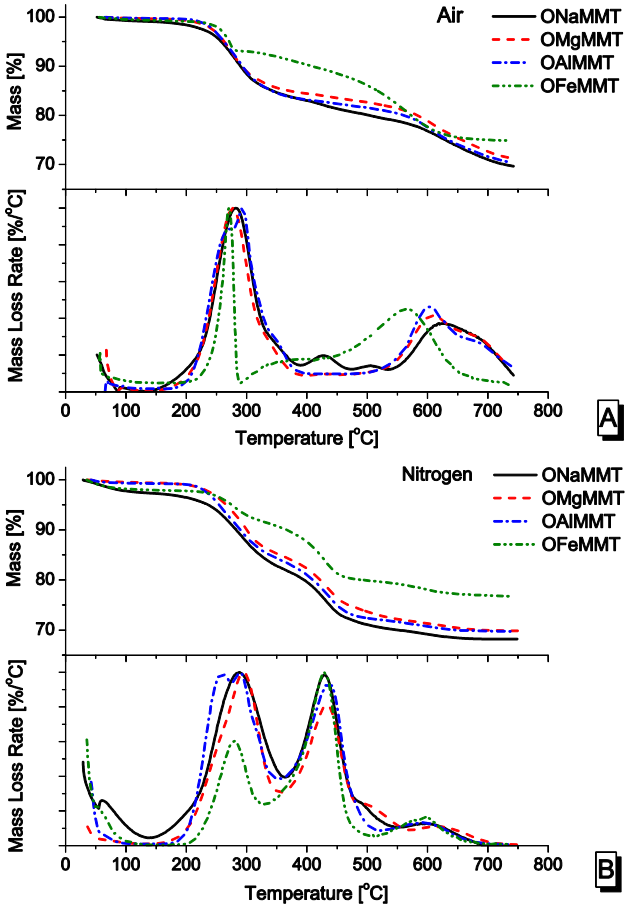

Figure 5. TG curves for $HDTMA^+$ modified clay samples in air (A) and nitrogen (B) atmospheres. Single column fitting image.

Although overall degradation onset for all OMI-clays is in line with widely accepted Hoffmann degradation mechanism (scheme 1) [35], they still show some distinctive features as a result of their corresponding Brønsted acidities and possible catalytic activity of dehydrated metal ions. OAlMMT not only showed quickest peak degradation (260 ^oC under nitrogen and 268 ^oC in air) but also showed a unique two-step mass loss between 260-295 ^oC, irrespective of test atmosphere. This effect may be attributed to the combination of three distinct phenomena, Brønsted acidity, catalytic effect of dehydrated Al^{3+} and Hoffman elimination. Figure 6A clearly indicates overlap for $T_{5\%}$ for OAlMMT and peak dehydration temperature of AlMMT which confirms conditions favoring (Brønsted) acidolysis of $HDTMA^+$. Although similar overlap was observed in case of FeMMT-OFeMMT pair (Figure 6B), presence of one derivative peak at 271 ^oC instead of twin peaks similar to AlMMT-OAlMMT pair indicate the characteristic difference between Al^{3+} and Fe^{3+} system. Relatively sharp mass loss in case of OFeMMT may be due to simultaneous effects of Brønsted acidity, catalytic effect of dehydrated Fe^{3+} ion on $HDTMA^+$ and Hoffman elimination. In the case of MgMMT, dehydration was almost complete below 210 ^oC and $T_{5\%}$ for OMgMMT (not shown separately). Hence, it may be inferred that the effect of Brønsted acidity is negligible in this case owing to the absence of hydration water. Further, it should also be noted that Mg^{2+} is relatively less reactive as compared to Al^{3+} or Fe^{3+} and therefore, the catalytic decomposition of quaternary ammonium ions with saturated long chain is absent.

Possible mechanism accounting for Brønsted acidity effect in case of OAlMMT and OFeMMT is depicted in scheme 2 where water from hydration spheres around Al^{3+} and Fe^{3+} act as a nucleophile which then abstracts acidic beta H^+ from $HDTMA^+$ to form carboanion and hydronium ion (H_3O^+). Subsequent rearrangements lead to formation of tertiary amine and alkene similar to Hoffman elimination. The negative charge, thus, generated on clay surface is neutralized by proton from H_3O^+ balancing the reaction. Thus, it is suggested that this additional effect of Brønsted acidity arising from hydration water in case of OAlMMT and OFeMMT is responsible for their quicker and distinctive thermal degradation patterns while generating same end products. Mass loss observed from TG analysis for all clays under both atmospheres are tabulated in Supporting Information (Table S1).

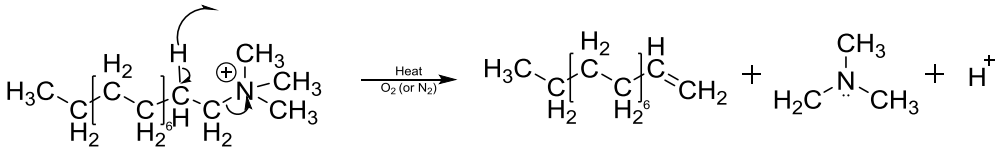

Scheme 1. Hoffman elimination mechanism for all OMI-clays. Double column fitting scheme.

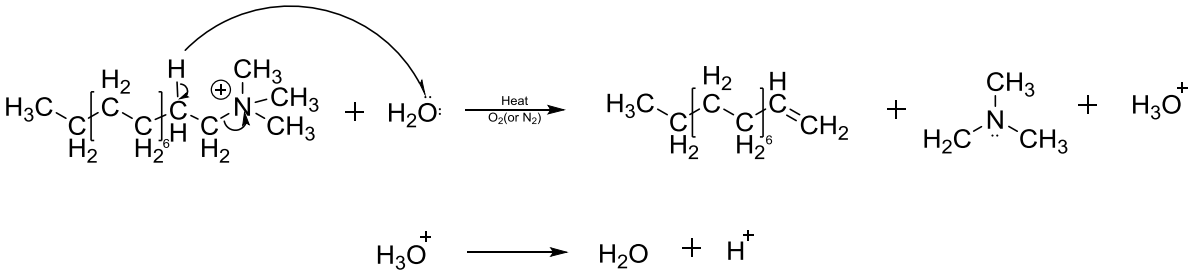

Scheme 2. Effect of Brønsted acidity on degradation of $HDTMA^+$ in OAlMMT and OFeMMT. Double column fitting scheme.

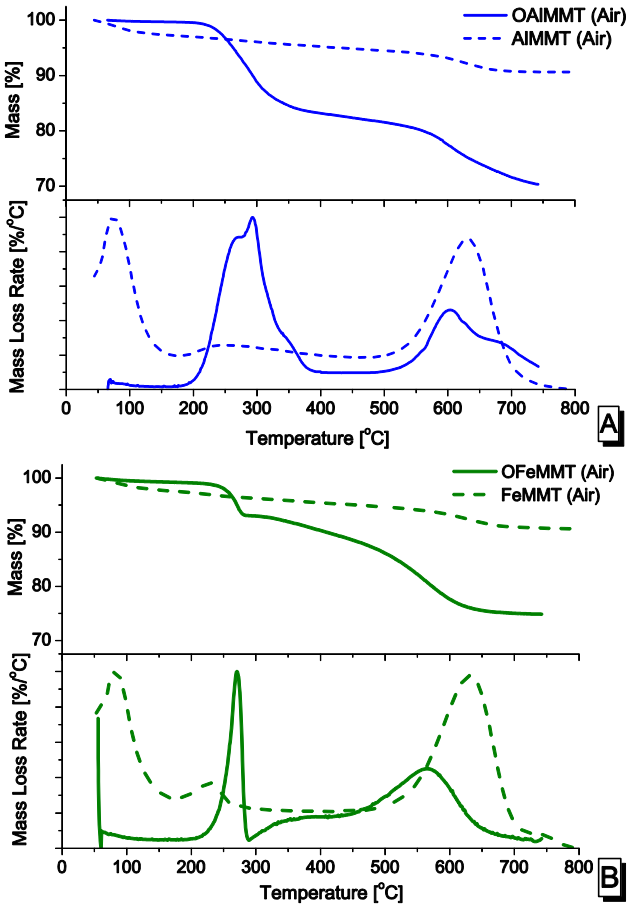

Figure 6. TG thermograms for Neat and HDTMA-Br modified clay samples in air atmosphere A) AlMMT B) FeMMT. Single column fitting image.

Further, it was observed that except for OFeMMT, each OMI-clay showed similar (11-16 wt%) mass loss between 260-300 ^oC irrespective of test atmosphere, whereas OFeMMT demonstrated mass loss of 6-7 wt%. This variation in case of OFeMMT was

related to lower quantity of surface adsorbed $HDTMA^+$ as seen from derivative weight loss peak at 270 ^oC for OFeMMT under inert atmosphere, which is also consistent with XRD and ICP-OES results. Nonetheless, in both atmospheres, AlMMT and FeMMT showed quicker onset of degradation of surface adsorbed $HDTMA^+$ owing to their inherent ionic nature and catalytic activity. However, OMgMMT showed slightly delayed peak degradation temperature, T_p, (297 ^oC) in inert atmosphere as compared to ONaMMT (291 ^oC). This might be of particular importance to polymer/clay nanocomposites as under fire conditions, surfactant and matrix decomposition occurs in oxygen-deprived atmosphere, essentially, pyrolytic conditions. This will be discussed further in a future communication.

Effect of Lewis Acidity: As opposed to a single observed effect of Brønsted acidity (on initial degradation of organoclays), Lewis acidity was found to affect three different processes, (i) kinetics of carbonaceous residue formation around 450 ^oC under oxidative conditions, (ii) oxidation stability of carbonaceous residue generated at temperatures above 550 ^oC and (iii) dehydroxylation temperatures of MI-clays at temperatures upside of 550 ^oC. The overlapping temperature regime for processes (ii) and (iii) further complicates the situation making it difficult to isolate the exact effect of metal ion on these processes.

Clay dehydroxylation essentially signifies loss of hydroxyl groups from octahedral layer in clay structure typically occurring at temperatures above 550 ^oC. The variations that are observed in the dehydroxylation temperatures of MI-clays (Figure 3) can be attributed to the variations in Lewis acid character and differences in interactions between exchangeable metal ions and surface hydroxyl groups present on clay surface.

Although OMI-clays when tested under inert conditions demonstrated similar temperatures, substantially different (lower) dehydroxylation temperatures were observed for tests carried out under oxidative atmosphere (Figure 5A) consolidating the simultaneous occurrence of residue oxidation and clay dehydration. An average drop of 15 ^{o}C was observed for all OMI-clays except for OFeMMT, which displayed a significant drop of 55 ^{o}C. These variations clearly suggest the combined effect of catalytic oxidation of carbonaceous residue from organic degradation as well as catalytic attack on clay surface by different metal ions. That is, amongst Na^{+}, Mg^{2+}, Al^{3+} and Fe^{3+}, Fe^{3+} has greater ability to catalytically oxidize carbonaceous residue and catalytically destroy the clay structure by assisting in dehydroxylation. This results in the formation of amorphous meta-montmorillonite[20]. In the following sections, clay residues at 450 ^{o}C and 750 ^{o}C were analyzed by FT-IR and XRD techniques to establish the effect of Lewis acidity.

Residue Analysis by FT-IR (air burnt samples)

As seen in Figure 7, FT-IR of residues (burnt at 750 ^{o}C) of all MI-clays, except FeMMT, displayed prominent reduction in peak intensities associated with OH-stretching (~3640, ~3450 cm^{-1}) and OH-bending vibrations (~1645 cm^{-1}) signifying the loss of surface water and water coordinated with interlayer cations [36]. For FeMMT, OH-stretch peak intensities were largely unchanged. The reasons for this are still unclear and require further investigation. But the shifts observed in bending vibration peak (~1645 cm^{-1}) in case of AlMMT and FeMMT to ~1608 and ~1622 cm^{-1},

respectively, can be attributed to the strong associations of metal ion (present at interlayer positions) with structural oxygen from dehydrated clay surface [37].

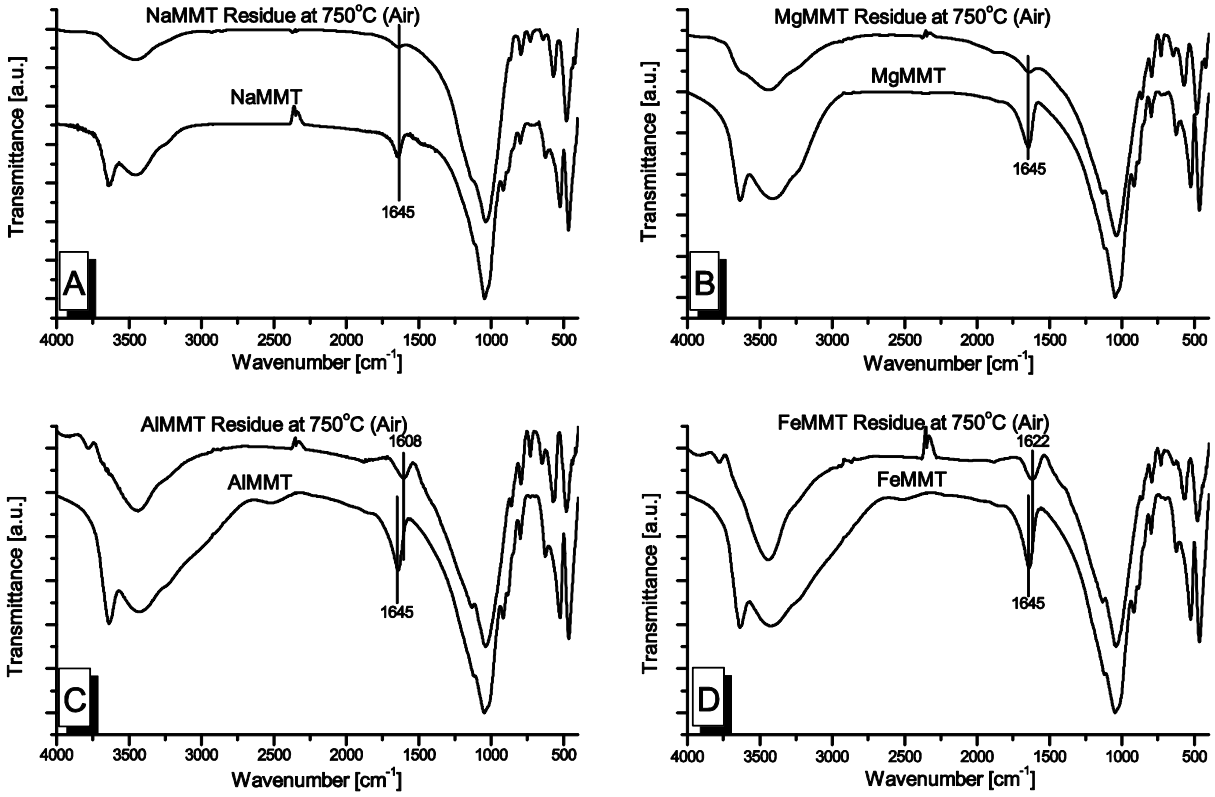

Figure 7. IR spectra for MI-clays and their residues tested in air at 750 ^{o}C. Double column fitting image.

In case of OMI-clay residues (burnt at 450 ^{o}C), intensities at ~3640 cm^{-1} and ~3450 cm^{-1} decreased as expected due to dehydration (Figure 8). Besides, a peak shift from original ~1645 cm^{-1} towards lower wavenumber was observed, similar to MI-clay. However, a sharp increase in peak intensity at 1615-1633 cm^{-1} is observed attributable to carbonaceous material consisting of C=C. New shoulder peaks observed around

1420-1480 cm^{-1} associated with -CH_2- are progressively stronger in the order of Na^{+}< Mg^{2+}< Al^{3+}< Fe^{3+}. Considering the presence of these absorption peaks at 1615-1633 cm^{-1} and 1420-1480 cm^{-1}, it can also be argued that aromatic structures are formed in accordance with degradation mechanism suggested by Bellucci et al. for long chain alkyl ammonium cation under oxidation [38] (Scheme 3). However, this mechanism does not account for formation of carbonyl groups either evolved as volatiles reported previously [35] or as observed in present case of OMI-clays.

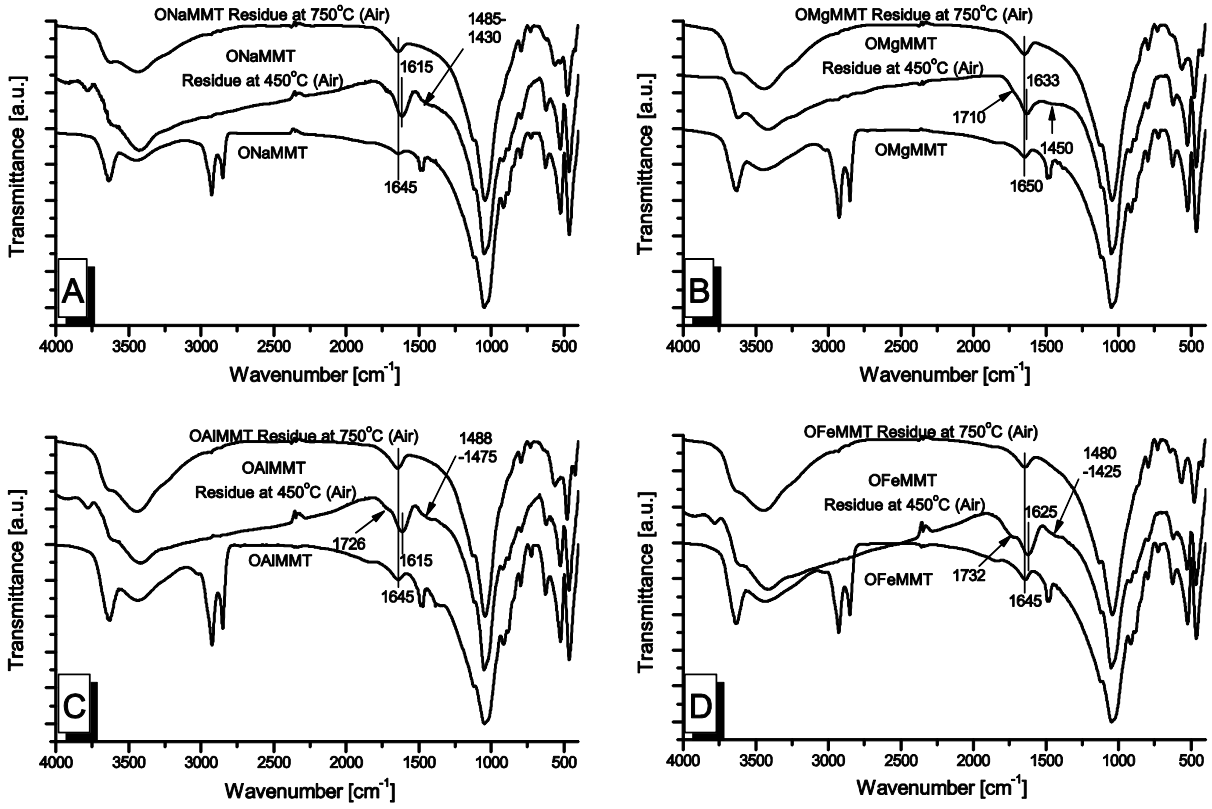

Figure 8. IR spectra for OMI-clays and their residues tested in air at 450 ^{o}C and 750 ^{o}C. Double column fitting image.

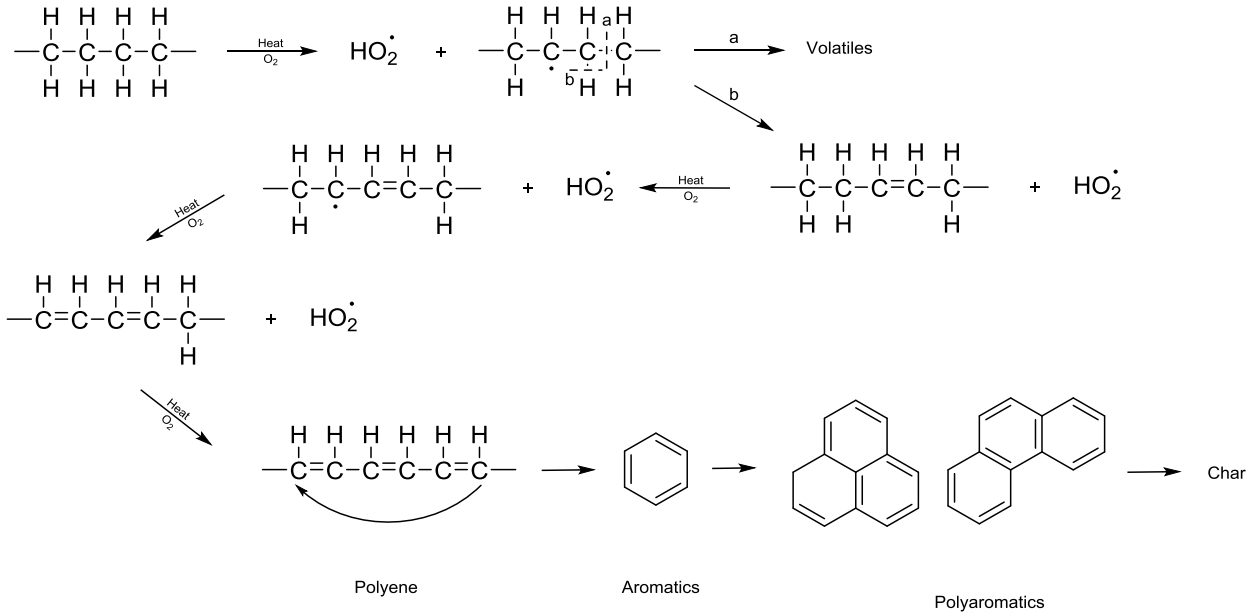

Scheme 3. Oxidative degradation mechanism for alkyl fragment from organic modifier as proposed by Bellucci et al [38]. Double column fitting scheme.

Xie et al. reported the generation of linear and branched aldehydes as observed from pyrolysis/GC-MS at 400 ^{o}C in case of MMT modified using trimethyl octadecylammonium chloride [35]. It was suggested that under confined lamellar conditions (experienced in collapsed clay structures), the presence of oxygen from clay surface along with catalytic activity of metal species from MMT structure, enabled the formation of aldehydes at higher temperatures following the oxidative cleavage under pyrolytic conditions. In the current work, shoulder peaks in OMI-clay residues at 450 ^{o}C around 1710-1735 cm^{-1}, generally associated with presence of C=O, are progressively stronger in the order of Na^{+}< Mg^{2+}< Al^{3+}< Fe^{3+}. This confirms the deviation from proposed hydrogen abstraction mechanism by Bellucci et al. under oxidative conditions. It also demonstrates the influence of metal ions in the generation of carbonyl groups in

organoclay residues. It is important to note that Xie et al. although confirmed the generation of aldehyde groups, they attributed their formation to catalytic oxidative reaction between degrading organic matter and oxygen from clay [35]. In current study, to investigate the role of oxygen from test atmosphere, OFeMMT was taken as representative sample as it displayed strongest shoulder corresponding to C=O. From Figure 9 it is evident that the shoulder for C=O is absent when test was performed under inert condition. This consolidates the influence of oxygen from test atmosphere. As a result, peroxy-based mechanism (Scheme 4) is proposed, which yields similar polyaromatic char products as reported before. In addition, carbonyl groups in volatiles or in residue can be generated.

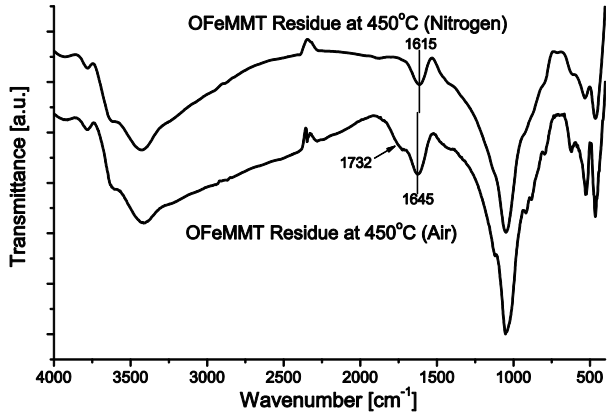

Figure 9. IR spectra for residues of OFeMMT tested in air and nitrogen at 450 ^{o}C.

Single column fitting image.

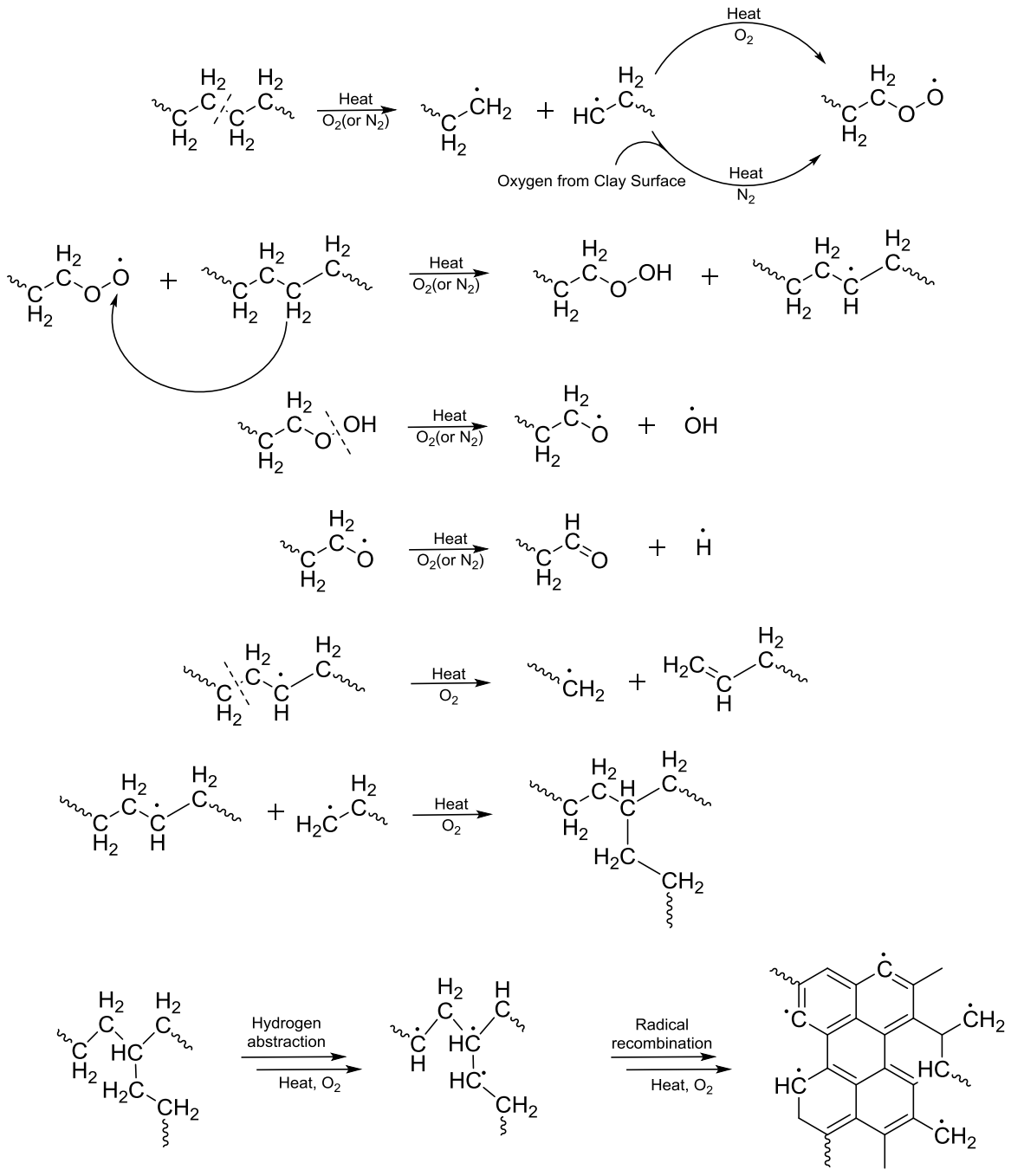

Scheme 4. Proposed peroxy-based degradation mechanism for alkyl fragment from organic modifier between 400-500 ^{o}C. Double column fitting scheme.

Formation of large quantities of highly reactive peroxy radicals under oxidative condition is crucial in determining the carbonaceous residue content. Higher are the quantities of these alkoxy, peroxy radicals, greater is the possibility for alkyl radical formation and their subsequent recombination, thus, lowering volatilization. Significantly lower quantities of such peroxy radicals can form under pyrolytic conditions as source of oxygen being surface adsorbed oxygen or surface hydroxyl groups on clay. As a result, essentially volatilization of organic matter predominates over radical recombination. The limited quantity of alkoxy radicals formed may yield volatile aldehydes as reported earlier.

Possible role of metal ion on rate of generation of carbonaceous residue under oxidative conditions is depicted in scheme 5. Presence of metal ions can accelerate the rate of decomposition of hydroperoxide generating oxy or peroxy organic radical[39]. This process is further accelerated at higher temperatures. Metal ion can either oxidize by donating one electron to hydroxyl radical or reduce by accepting one electron from proton radical, generating corresponding ions. Although this phenomenon can occur under any atmosphere, intuitively it should be more prominent under oxygen atmosphere due to abundance of alkyl hydroperoxide. It is known that higher valence ions show more prominent effect which might be correlated to stronger C=O absorption peak in their corresponding OMI-clay residue IR spectra. Hence, presence of metal cations can uniquely affect the rate of generation of carbonaceous residue starting at 400 ^{o}C based on their inherent catalytic characteristics.

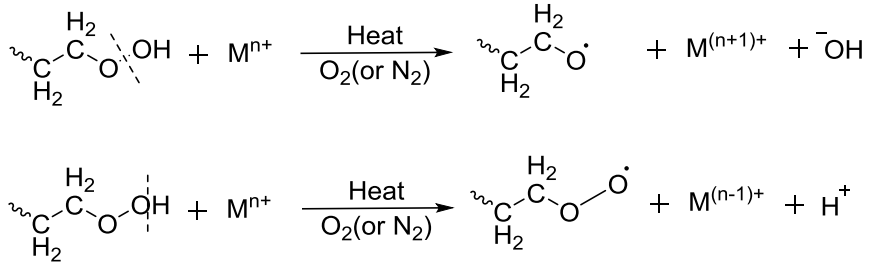

Scheme 5. Effect of metal ions on decomposition of hydroperoxides yielding highly reactive organic oxy or peroxy radicals [39]. Double column fitting scheme.

It was suggested that oxidative degradation of alkyl chains by forming peroxy groups [40,41] is more prominent at temperatures below 200 ^{o}C whereas at temperature above 250 ^{o}C hydrogen abstraction by oxygen molecule becomes more prominent as in case of Scheme 3. However, presence of noticeable C=O absorption peaks and presence of aldehydes suggest that confinement effect from partially collapsed clay, catalytic effect from dehydrated metal ions and Lewis acid sites from clay edges may significantly influence the overall oxidative degradation mechanism and may favor one over other. Possibility of simultaneous occurrence of both degradation routes in Scheme 3 and 4 may not be refuted. It is important to note the difference between thermo-oxidative degradation of alkylammonium modifiers with and without hydroxyl groups where generation of aldehydes have well established mechanism [42] different from one discussed here.

Although exact nature of this carbonaceous matter is currently not investigated, but it can be concluded that presence of different metal ions at exchange positions alter the degradation kinetics of organic modifier. By comparing the IR spectra for MI-clay

residues and OMI-clay residues at 750 ^{o}C it is evident that the peak intensities at 1615-1633 cm^{-1} are lowered and additional shoulders (1420-1480 cm^{-1} and 1710-1735 cm^{-1}) are absent. This confirms the loss of carbonaceous matter when continued heating above 450 ^{o}C and up to 750 ^{o}C.

Residue Analysis by XRD (air burned samples)

To further substantiate the role of Lewis acidity as seen from TG analysis results (under oxidative condition), XRD analysis for respective residues was carried out to verify the presence of any carbonaceous matter sandwiched between collapsed clay platelets that can be observed through increased interlayer distances. For comparison purpose, interlayer spacing for pristine NaMMT and its residues at 450 ^{o}C and 750 ^{o}C were presented in Figure 10. Apparently 450 ^{o}C was sufficient enough temperature for complete dehydration of NaMMT causing a complete platelet collapse from 12.1 Å to 9.8 Å. Further heating up to 750 ^{o}C, beyond its dehydroxylation temperature range of 550-675 ^{o}C, had no impact on the final d_{001} of NaMMT residue. Conversely, as shown in Figure 11A, instead of complete platelet collapse to 9.8 Å, residues of all OMI-clays at 450 ^{o}C displayed only partial collapse from ~18 Å to 13 Å which in conjunction with TGA results confirm presence of carbonaceous matter between interlayer of clay platelets [43]. However, absence of any peaks corresponding to well-structured carbon suggests that the carbonaceous matter formed is of amorphous nature or its content is below the detection limit. Figure 12 depicts schematic representation of formation of residual carbonaceous matter through thermal degradation of OMI-clays.

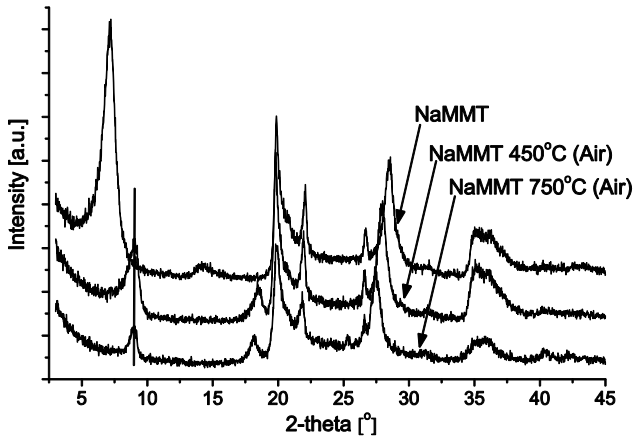

Figure 10. XRD of residue of pristine NaMMT tested under air atmosphere. Single column fitting image.

Interesting effects on stability of carbonaceous matter were observed for OMI-clays while studying XRD patterns for their residues at 750 ^{o}C (Figure 11B). Despite the near complete collapse of all residues as a result of oxidation of carbonaceous matter [44,45], there seems to be minor variations in their final d_{001} spacing (shown in inset). These variations could be attributed to metal ions present in different OMI-clays and their catalytic effects on delaying the oxidation of carbonaceous matter. Amongst OMI-clay residues, OFeMMT achieved complete oxidation/dehydroxylation by 750 ^{o}C as evident from the overlapping d_{001} peaks for residues of NaMMT (~9.8 Å) and OFeMMT (~10 Å). Thus, it was suggested that catalytic nature of Fe^{3+} can significantly reduce the final char yield by assisting oxidation. Hsiao et al. observed similar behavior of Fe^{3+} resulting in lower char as a result of catalytically assisted combustion at lower temperatures[30]. A shift in d_{001} to ~10.6 Å for ONaMMT, OMgMMT and OAlMMT as against ~9.8 Å for NaMMT is a result of presence of residual carbonaceous content. It

can be concluded that Mg^{2+} and Al^{3+} ions from these clays retard oxidation of said carbonaceous content, in turn resulting in incomplete oxidation (even up to 750 ^{o}C). The delay in oxidation can be correlated to Figure 5A, where peak mass loss rate and the tail in its broad temperature peak between 550-750 ^{o}C is quite evident for OMI-clays. Song et al. also reported a noticeable improvement in performance of charring catalyst through introduction of magnesium. Magnesium was believed to improve the utilization of nickel, a known carbonizing catalyst [46].

In order to verify the complete loss of $HDTMA^{+}$ when heated up to 450 ^{o}C as seen from the TG results for inert atmosphere (Figure 5B), a representative sample, OFeMMT, and its residues at 450 ^{o}C and 750 ^{o}C were analyzed using XRD. Complete collapse of clay platelets representing absence of carbonaceous matter in residues was observed for clay residue at 450 ^{o}C, thus, verifying the reason provided. Corresponding XRD curves comparing samples tested in air and nitrogen and residues at 450 ^{o}C and 750 ^{o}C are given in Supporting Information (Figure S3)

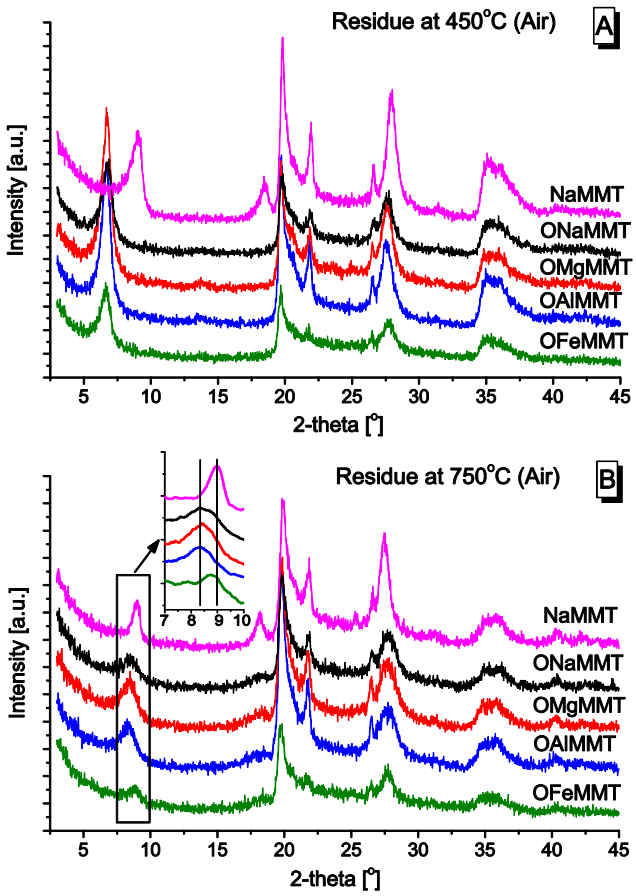

Figure 11. XRD of residue of CTAB modified clay samples tested in air at 450 ^{o}C (A) and 750 ^{o}C (B). Single column fitting image.

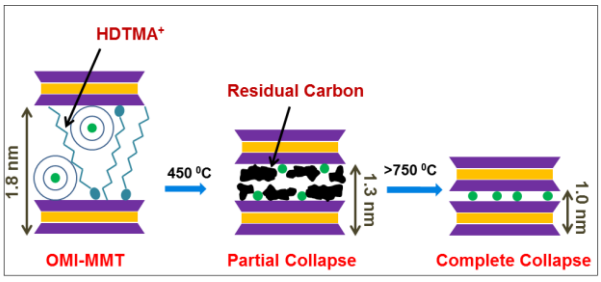

Figure 12. Schematic representation of formation of residual carbon at clay interlayers affecting d_{001} spacing for OMI-clay residues at 450 ^{o}C. Exact temperature above 750 ^{o}C

for complete collapse depends on oxidation stability of residual carbon in presence of different metal ions (Na^{+}, Mg^{2+}, Al^{3+} or Fe^{3+}). Single column fitting image.

In short, it can be concluded that final char content is governed by inherent concentrations of Mg^{2+}, Al^{3+} and Fe^{3+} in MMTs as they affect its Lewis acid character. For example, Fe^{3+} rich NaMMT reduces the char content, while the sample containing higher Mg^{2+} or Al^{3+} gives opposite effect. Thus, it becomes important to compare ion percentage from MMT used in different studies before generalizing any effects. Generally, owing to much lower contents of these ions in MMTs than those used in this study, their effect on degradation of polymer matrix is overlooked.

Finally, to further consolidate TGA and XRD results, CHN technique was employed for clays and their residues at 450 ^{o}C and 750 ^{o}C. As a representative samples, carbon content (%) for ONaMMT and OAlMMT are tabulated in Supporting Information, Table S2. It is quite evident that clay residues at 450 ^{o}C have significant carbon content whereas clay residues at 750 ^{o}C display only trace amounts as a result of loss due to oxidation, supporting the argument made in previous section.

CONCLUSIONS

A better understanding was achieved regarding the catalytic effects of individual metal ions (Mg^{2+}, Al^{3+} and Fe^{3+}), inherently present in varied proportions in MMT chemical structure, on the thermal degradation of organic modifier, $HDTMA^{+}$. The catalytic activity

was seen to be a combined effect of Bronsted and Lewis acid characters associated with these metal ions. Significant findings include:

1. Difference in Brønsted acidity, as a result of water coordinated with different interlayer MIs, govern the onset of $HDTMA^+$ degradation.
2. Lewis acidity for OMI-clays can affect the rate of generation of carbonaceous content in residue depending on inherent metal ion characteristics following the mechanism proposed.
3. Lewis acidity for OMI-clays affects the oxidation stability of carbonaceous content in residue. Although both Al^{3+} and Fe^{3+} exchanged clays demonstrated lower degradation onset temperatures ($T_{5\%}$), Al^{3+} showed more pronounced effect on initial $HDTMA^+$ degradation mechanism. OMgMMT showed delayed peak degradation for $HDTMA^+$ under inert conditions owing to its lower catalytic action towards $HDTMA^+$.
4. Significant reduction in MMT dehydroxylation temperatures were observed to be dependent on Lewis acid character varying amongst OMI-clays.
5. XRD analysis for residues indicate that while Fe^{3+} ions from OFeMMT predominantly influenced oxidation stability of carbonaceous content while presence of Mg^{2+} and Al^{3+} resulted into delayed oxidation of carbonaceous matter.

ACKNOWLEDGEMENTS

AD acknowledges the Start-up-Grant from Nanyang Technological University and the Academic Research Fund Tier-1 (RG45/11) from the Singapore's Ministry of Education for financially supporting parts of this research.

REFERENCES

1] M. Bartholmai, B. Schartel, Polym. Adv. Technol. 15 (2004) 355-364.

2] A.B. Morgan, L.L. Chu, J.D. Harris, Fire Mater. 29 (2005) 213-229.

3] N. Huang, J. He, J. Du, J. Wang, J. Fire Sci. 30 (2012) 256-269.

4] J.W.Gilman, Appl. Clay Sci. 15 (1999) 31-49.

5] H. Qin, S. Zhang, C. Zhao, M. Feng, M. Yang, Z. Shu, S. Yang, Polym. Degrad. Stab. 85 (2004) 807-813.

6] R. Davis, J. Gilman, D. VanderHart, Polym. Degrad. Stab. 79 (2003) 111-121.

7] K. Prakalathan, S. Mohanty, S. Nayak, J. Reinf. Plast. Compos. 31 (2012) 1300-1310.

8] Y. Cai, F. Huang, Q. Wei, L. Song, Y. Hu, Y. Ye, Y. Xu, W. Gao, Polym. Degrad. Stab. 93 (2008) 2180-2185.

9] C. Deng, J. Zhao, C.-L. Deng, Q. Lv, L. Chen, and Y.-Z. Wang, Polym. Degrad. Stab. 103 (2014) 1-10.

10] Z. Wang, X. Du, H. Yu, Z. Jiang, J. Liu, and T. Tang, Polymer 50 (2009) 5794-5802.

11] B. Schartel, A. Weiß, Fire Mater. 34 (2010) 217-235.

12] A. Fina, F. Cuttica, G. Camino, Polym. Degrad. Stab. 97 (2012) 2619-2626.

13] J. Humphrey, D. Boyd (Eds.), Clay; Types, Properties and Uses, Nova Science Publishers Inc., New York, 2011.

14] C. Ravindra Reddy, G. Nagendrappa, B. Jai Prakash, Catal. Commun. 8 (2007) 241-246.

15] C. Breen, A. Moronta, J. Phys. Chem. B 104 (2000) 2702-2708.

16] M. Dong, X. Gu, S. Zhang, H. Li, P. Jiang, Indus. Eng. Chem. Res. 52 (2013) 9145-9154.

17] F. Bergaya, G. Lagaly (Eds.), Handbook of Clay Science Part A: Fundamentals, second ed., Elsevier, Oxford, 2013.
18] C. Rhodes, D. Brown, J. Chem. Soc. Faraday Transactions 91 (1995) 1031-1035.
19] P. Misaelides, F. Macasek, T. Pinnavaia, C. Colella, Natural Microporous Materials in Environmental Technology, Kluwer Academics Publishers, Dordrecht, 1999.
20] V. Balek, Z. Málek, S. Yariv, G. Matuschek, J. Therm. Anal. Calorim. 56 (1999) 67-76.
21] Y. Li, X. Wang, J. Wang, J. Therm. Anal. Calorim. 110 (2012) 1199-1206.
22] S. Hawkes, J. Chem. Edu. 73 (1996) 516.
23] I. Persson, Pure Appl. Chem. 82 (2010) 1901-1917.
24] S. Lee, P. Fenter, C. Park, N. Sturchio, K. Nagy, Langmuir 26 (2010) 16647-16651.
25] W. Grzybkowski, Polish J. Environ. Studies 15 (2006) 655-663.
26] V. Balek, M. Beneŝ, J. Ŝubrt, J. Pérez-Rodriguez, P. Sánchez-Jiménez, L. Pérez-Maqueda, J. Pascual-Cosp, J. Therm. Anal. Calorim. 92 (2008) 191-197.
27] P. Wallis, A. Chaffee, W. Gates, A. Patti, J. Scott, Langmuir 26 (2009) 4258-4265.
28] G. Wulfsberg, Inorganic Chemistry, University Science Books, Sausalito, 2000.
29] B. Teppen, V. Aggarwal, Clay Clay Miner. 55 (2007) 119-130.
30] P. Nawani, M. Gelfer, B. Hsiao, A. Frenkel, J. Gilman, S. Khalid, Langmuir 23 (2007) 9808-9815.
31] R. Calvet, Hydration de la montmorillonite et diffusion des cations compensateurs. PhD Thesis, University of Paris VI (Pierre et Marie Curie), Ann Arbor, France, 1972.
32] J. Fripiat, M. Cruz-Cumplido, Annu. Rev. Earth Planet Sci. 2 (1974) 239-256.
33] C. Breen, A. Deane, J. Flynn, Clay Miner. 22 (1987) 169-178.
34] B. Wang, M. Zhou, Z. Rozynek, J. Fossum, J. Mater. Chem. 19 (2009) 1816-1828.
35] W. Xie, Z. Gao, W. Pan, D. Hunter, A. Singh, R. Vaia, Chem. Mater. 13 (2001) 2979-2990.
36]J. Madejova, H. Palkova, P. Komadel, IR spectroscopy of clay minerals and clay nanocomposites, in: J. Yarwood, R. Douthwaite, S. Duckett (Eds.), Spectroscopic Properties of Inorganic and Organometallic Compounds, RSC Publishing, Cambridge, 2010, p. 22-71.
37] J. Bishop, C. Pieters, J. Edwards, Clay Clay Miner. 42 (1994) 702-716.

38] F. Bellucci, G. Camino, A. Frache, A. Sarra, Polym. Degrad. Stab. 92 (2007) 425-436.
39] H. Zweifel, Stabilization of Polymeric Materials, Springer-Verlag Berlin Heidelberg, Berlin Heidelberg, 1998.
40] S. Benson, P. Nangia, Acc. Chem. Res. 12 (1979) 223-228.
41] S. Benson, Prog. Ener. Combus. Sci. 7 (1981) 125-134.
42] J. Cervantes-Uc, J. Cauich-Rodríguez, H. Vázquez-Torres, L. Garfias-Mesías, D. Paul, Thermochim. Acta 457 (2007) 92-102.
43] W. Xie, Z. Gao, K. Liu, W. Pan, R. Vaia, D. Hunter, A. Singh, Thermochim. Acta 367–368 (2001) 339-350.
44] P. Nawani, P. Desai, M. Lundwall, M. Gelfer, B. Hsiao, M. Rafailovich, A. Frenkel, A. Tsou, J. Gilman, S. Khalid, Polymer 48 (2007) 827-840.
45] C. Chou, J. McAtee Jr., Clay Clay Miner. 17 (1969) 339-346.
46] R. Song, Y. Fu, B. Li, J. Appl. Polym. Sci. 129 (2013) 138-144.

Elucidating the catalytic effect of metal ions in montmorillonite on thermal degradation of organic modifier

Indraneel S Zope[1], Aravind Dasari[1,*], Giovanni Camino[2]

[1]School of Materials Science & Engineering (Blk N4.1), Nanyang Technological University,

50 Nanyang Avenue, Singapore 639798

[2]Dipartimento di Scienza Applicata e Tecnologia, Politecnico di Torino sede di Alessandria, INSTM research unit, Viale Teresa Michel 5, 15100 Alessandria, Italy

Supporting Information

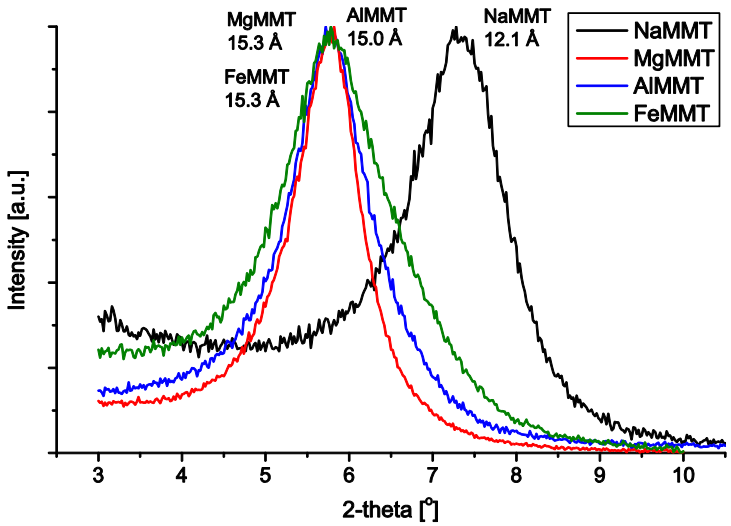

Figure S1. XRD for MI-clays.

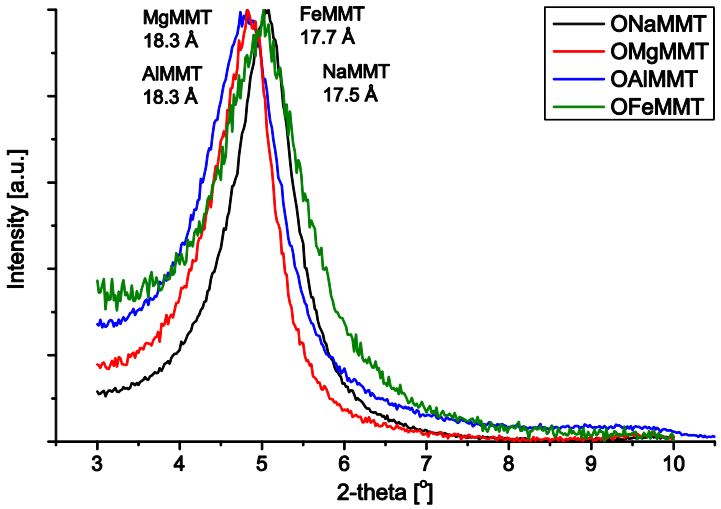

Figure S2. XRD for OMI-clays.

Table S1. TG analysis for OMI-clays in air and nitrogen.

	ONaMMT		OMgMMT		OAlMMT		OFeMMT	
	T (°C)	% wt loss	T (°C)	% wt loss	T (°C)	% wt loss	T (°C)	% wt loss
Air	283	15.6	278	15.2	268 293	7.1 9.4	271	6.3
	400-500	4.1					300-430	3.9
	620	9.6	609	13.2	606	12.9	565	14.3
Res @ 450	81.8		84.8		83.5		89.9	
Res @ 750	69.7		71.3		70.4		74.9	
N_2	291	14.3	297	12.4	260 289	7.3 7.9	273	6.9
	431	12.4	432 460-550	11.7 3	435	12.0	423	11.4
	596	2.4	613	2	589	2.4	618	2.9
Res @ 450	73.5		75.3		74.3		80.8	
Res @ 750	68.2		69.4		69.6		76.7	

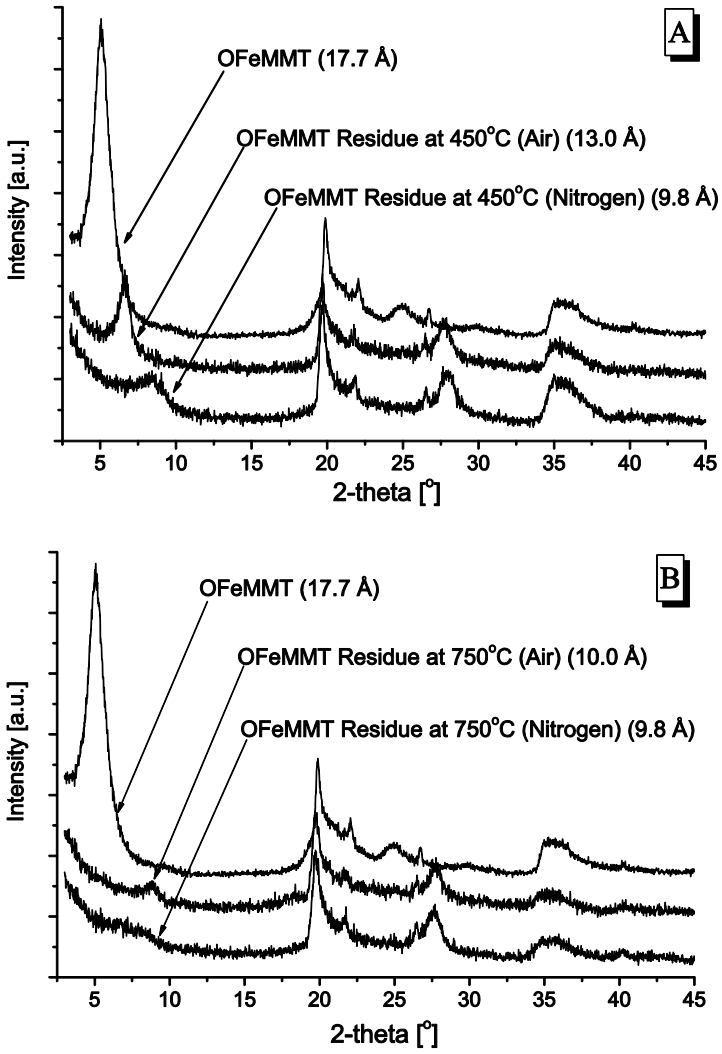

Figure S3. XRD of OFeMMT and its residues tested in air and nitrogen at 450 ^{o}C (A) and 750 ^{o}C (B).

Table S2. Carbon content (%) in ONaMMT and OAlMMT and their residues at 450 ^{o}C and 750 ^{o}C as noted from CHN technique. (Average values from triplicate results).

	ONaMMT	OAlMMT
25 ^{o}C	31.76	31.77
450 ^{o}C	14.75	13.79
750 ^{o}C	0.53	0.64